nature photonics

LETTERS

PUBLISHED ONLINE: 20 JANUARY 2013 | DOI: 10.1038/NPHOTON.2012.341

Realization of three-dimensional guiding of photons in photonic crystals

Kenji Ishizaki, Masaki Koumura, Katsuyoshi Suzuki, Kou Gondaira and Susumu Noda*

Three-dimensional photonic crystals[1–10] are expected to provide a fundamental building block for the realization of three-dimensional manipulation of photons. However, because of the lack of systematic design principles to precisely control bending and guiding in three dimensions, as well as advancements in the fabrication technology necessary for the realization of large-area, defect-free three-dimensional photonic crystals, the arbitrary three-dimensional manipulation of photons has yet to be demonstrated. Here, we develop a new design concept for three-dimensional waveguides and bends, and realize it experimentally in silicon three-dimensional photonic crystals. We demonstrate clear three-dimensional optical guiding phenomena, in which light is incident on the crystal from one side, is bent vertically and horizontally (and is even split into two or trapped by an intermediate nanocavity), and is finally emitted from the other side of the crystal. These results will open the door to the realization of three-dimensional optical chips with various functionalities.

To date, realizing on-demand three-dimensional (3D) guiding of photons in 3D photonic crystals has proven to be quite challenging. One approach based on an inverse-opal 3D photonic crystal combined with lithography[5] failed to demonstrate such 3D optical guiding. In that research, neither the design strategy nor quantitative analysis of the experimental results were investigated, and a number of unintentional defects and disorders were introduced. Another approach based on stacked-stripe (or woodpile) 3D crystals[9,10] also failed due to the lack of a design concept and insufficient vertical confinement. In relation to design, theoretical proposals have been made for connecting horizontal waveguides in different layers within 2D–3D hybrid photonic-crystal systems through an intermediate short-length vertical-waveguide cavity[11,12]. However, more comprehensive designs are necessary that have a direct connection between horizontal and vertical waveguides, vertical and vertical waveguides, and so on.

We begin by describing a design strategy for the 3D guiding of photons. Stacked-stripe (or woodpile) 3D crystals[1] are used as the basic crystalline structure, as they have superior properties among the various crystals developed to date[1]. There have been a few reports on the design of waveguides in stacked-stripe 3D crystals[9,12–15]. Representative examples of horizontal and vertical waveguides are shown in Fig. 1a,b as schematic structures, together with their dispersion characteristics as calculated by the 3D finite-difference time-domain (FDTD) method with the width and thickness of the dielectric stripes set at $0.3a$ and $\sqrt{2}\,a/4$ (where a is the stripe period), respectively. The horizontal waveguide (Fig. 1a), constructed with one stripe missing inside the crystal, has single-mode characteristics over a wide band in the normalized frequency range of $\sim$0.340–0.375c/a. The vertical waveguide (Fig. 1b), in which stripes are partially removed (width of $1.0a$) in the vertical direction, is single mode in only a very narrow band, and has significantly different dispersion characteristics. These differences in the dispersion characteristics make it difficult to connect the two waveguides, thereby preventing the realization of 3D guiding of photons. Accordingly, there is a need for a vertical waveguide design with wideband single-mode behaviour comparable with that in Fig. 1a.

A comparison of the waveguides shown in Fig. 1a,b reveals that the horizontal waveguide is oriented along the [110] direction of the photonic-crystal structure, whereas the vertical waveguide is oriented along the [001] direction. This difference from the viewpoint of crystalline symmetry might have induced the serious mismatch in the dispersion characteristics. If the vertical waveguide could somehow be oriented along a direction identical to that of the horizontal waveguide [110], the dispersion characteristics would be expected to be similar. Figure 1c shows an example of such a waveguide in which partially missing stripes (or point defects) are stacked obliquely along the [101] direction, which is equivalent to the [110] direction. The calculated dispersion characteristics of this oblique waveguide in Fig. 1c are indeed found to be similar to those of the horizontal waveguide (Fig. 1a). (The effects of the defect widths on the dispersion characteristics are described in Supplementary Section SI.) We also confirmed that this oblique waveguide can function as a vertical waveguide, as shown in Fig. 1d, although it is tilted 45° from the direction normal to the crystal surface or the (001) plane. Figure 1d illustrates the magnetic field distribution of the wave propagating from the input to the output side of the obliquely oriented waveguide formed in a 3D photonic crystal with 16 stacked-stripe layers, with the focused Gaussian beam incident on the waveguide. Figure 1e shows the calculated transmission spectra with and without the waveguide. Because of the finite number of stacked-stripe layers, a background transmission intensity with a magnitude of 10^{-7} to 10^{-6} remains. When the waveguide is introduced, the transmittance is found to increase significantly (by a factor of 10^3 to 10^4), which clearly indicates the onset of vertical transmission. A detailed discussion of the transmission characteristics, including coupling losses and considerations for improving the transmittance, is provided in Supplementary Section SII.

We next discuss connecting the individual waveguides so as to bend light in three dimensions. As the dispersion characteristics of the horizontal and newly designed oblique (or vertically oriented) waveguides are identical, the design of the bend is critical. The strategy here is to construct a low-quality-factor cavity that will act as an intermediary to smoothly connect the waveguides[13,16–18]. Figure 2a presents a schematic view of the bending between the horizontal and oblique waveguides. Three possible structures for the connection are considered: one in which both waveguides are connected without any adjustment at the connecting point (Fig. 2b), another where one waveguide (horizontal) has a small extension at the connecting point (Fig. 2c), and one where both waveguides have extensions at the connecting point (Fig. 2d). (The lengths of the extended parts in Fig. 2c,d are set at $1.0a$ and $0.5a$, respectively.)

Department of Electronic Science and Engineering, Kyoto University, Kyoto 615-8510, Japan. *e-mail: snoda@kuee.kyoto-u.ac.jp

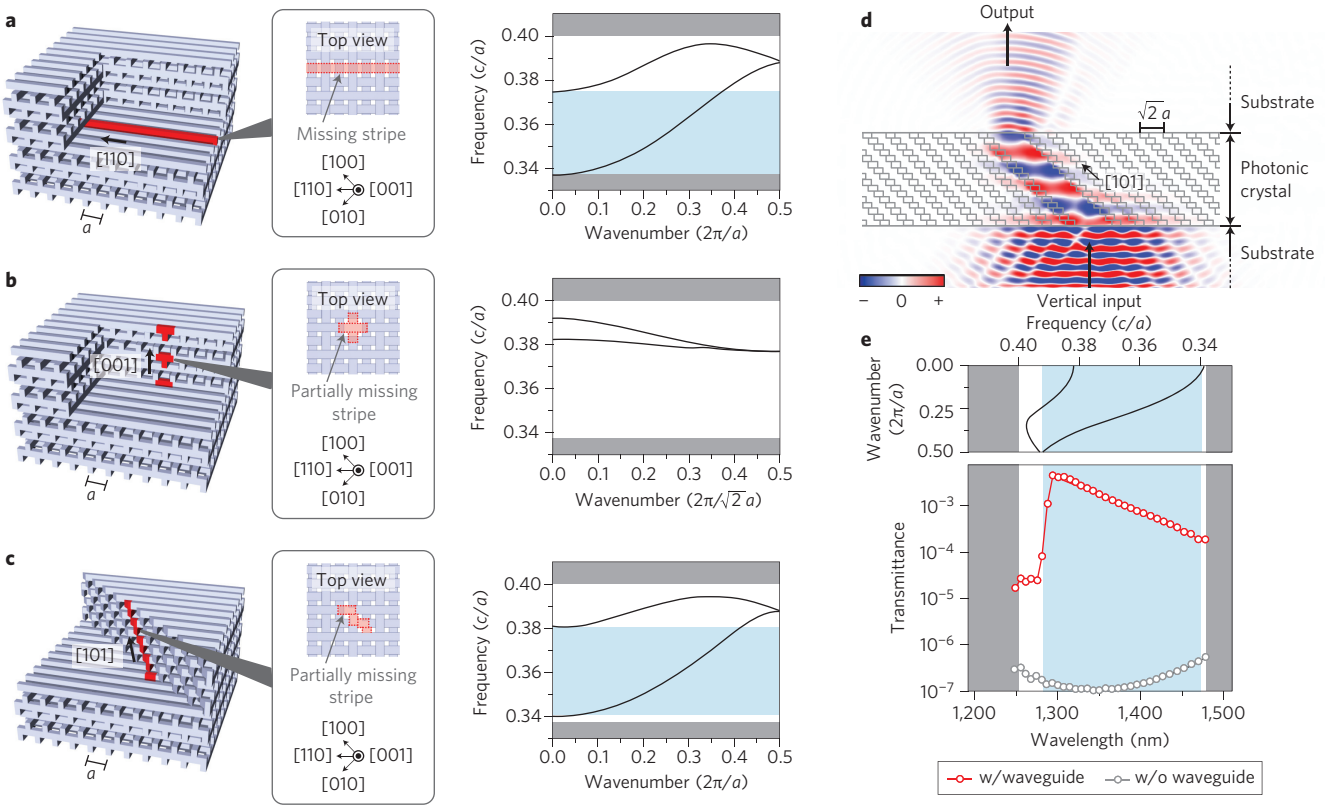

Figure 1 | Fundamental waveguides for 3D light guiding. a,**b**, Schematic and dispersion characteristics of previously designed horizontal and vertical waveguides[9,13]. **c**, Schematic and dispersion characteristics of a newly designed oblique (or vertically oriented) waveguide. The width of the partially missing stripe is 0.6*a*. **d**, Magnetic field distribution ([100]-directional component) of the propagating mode through the new oblique waveguide, in which the incident focused Gaussian beam has a full-width at half-maximum of 4.6*a* and frequency of 0.360*c*/*a*. **e**, Transmission spectra with and without the new oblique waveguide, assuming the utilization of objective lenses with numerical apertures of 0.42 and 0.70 for the incident and output sides, respectively.

The calculated loss due to the bend for the common single-mode frequency region of the horizontal and oblique waveguides is shown in Fig. 2b–d. The structure that minimizes the bending loss over the bandwidth of interest is obtained when only one of the two connecting waveguides is extended (Fig. 2c). In contrast, in the case of the connection between oblique waveguides, the best result is achieved when both waveguides have an equal extension of 0.50*a* (Fig. 2e). This configuration is also suitable for the case of two connecting horizontal waveguides, as previously discussed[1,13] (see also Fig. 2f, in which both waveguides have an equal extension of 0.35*a*). These results indicate that we have successfully produced systematic designs for connections between horizontal and oblique waveguides, and between oblique (or horizontal) waveguides.

We then proceeded to fabricate the designed structure in order to demonstrate 3D optical-guiding phenomena. We used a wafer-bonding approach based on the alignment and stacking of 2D stripe structures[1,19,20], the process sequence of which is summarized in Supplementary Section SIII. In the present work we newly introduce an automatic alignment system based on pattern recognition for the quantitative estimation of misalignment (Supplementary Section SIV). In this way we could realize very highly accurate and reproducible alignment and stacking, which is necessary for creating arbitrary multilayered structures.

Using this automatic alignment and stacking method, we created 3D crystals with various artificial defects. Figure 3a presents a scanning electron microscopy (SEM) image of a 3D crystal into which an oblique waveguide has been introduced with 16 stacked-stripe layers. Individual missing stripes (or point defects) are successfully stacked in the oblique direction, where the period *a* of the parallel stripes and the width of the missing stripe are set at 500 nm (= *a*) and 300 nm (= 0.6*a*), respectively. We initially measured the transmission spectra of the 3D crystal with no artificial defects introduced, and confirmed that the fabricated photonic crystals had full 3D bandgaps at wavelengths of 1,220–1,500 nm (Supplementary Section SV). We next measured the optical transmission characteristics of vertical (oblique) waveguides (Fig. 3a) and obtained the results shown in Fig. 3b. (The experimental setup is described in detail in Supplementary Section SVI.) The transmission increased in the wavelength range 1,250–1,450 nm. Moreover, by changing the widths of the point defects, it was shown that the transmission band could be tuned (Fig. 3c). These results agree well with the calculated results shown in Fig. 1e and Supplementary Fig. S1. The small wavelength dependence of the transmittance in the experiment (Fig. 3b) compared with that of the theoretical analysis (Fig. 1e) may be the result of a small misalignment during the fabrication process that may have modified the field pattern at the surfaces of the waveguide, thus affecting the coupling (or collection) efficiency between the incident (or output) light and the objective lens (also see discussions in Supplementary Section SII). We may therefore say that the incident light is coupled well to the vertical (oblique) waveguide from the bottom of the crystal and propagates through the waveguide.

We next connected an oblique waveguide, a horizontal waveguide and another oblique waveguide in sequence (Fig. 3d). The SEM image in Fig. 3e shows the halfway stage of the fabrication process, which would be followed by the remaining half of the 3D crystal being placed on this structure to finish the composite waveguide system. (The horizontal waveguide was extended by a length

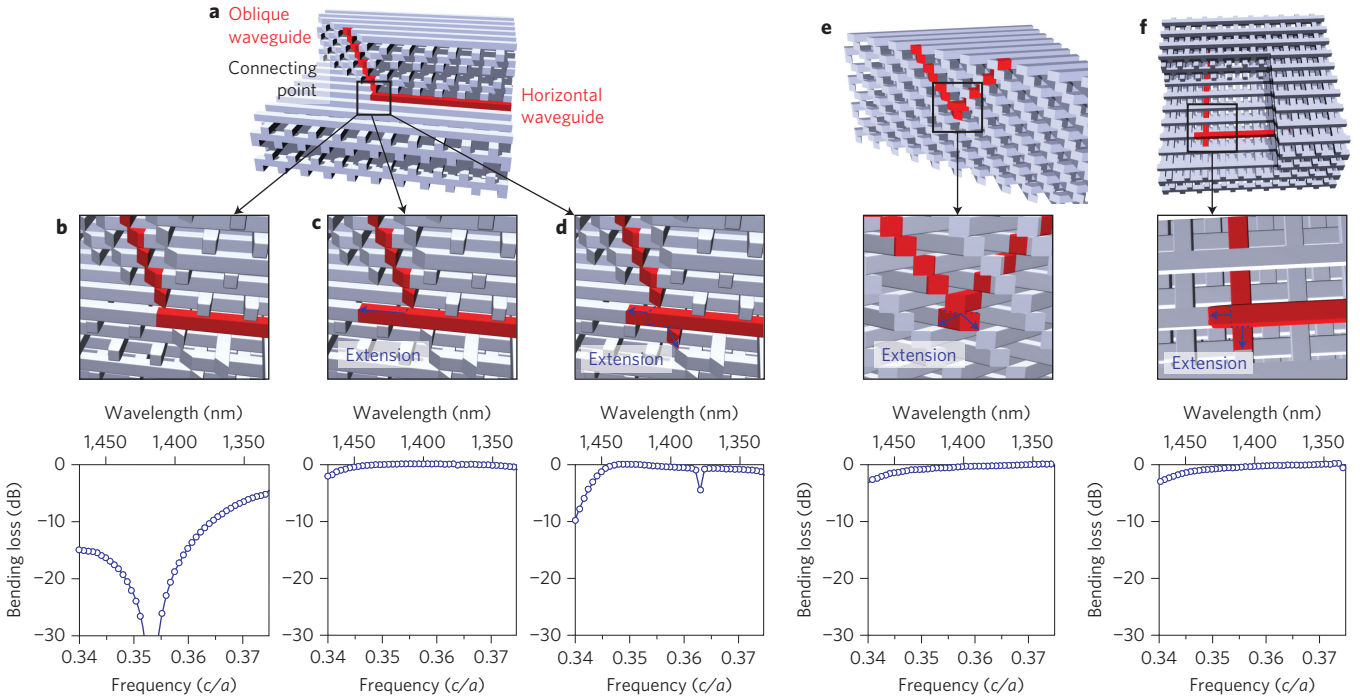

Figure 2 | Connection of individual waveguides to bend light. a, Schematic image of the connection of horizontal and oblique waveguides. **b**–**d**, Possible connecting structures and calculated bending losses at the connecting point. In the panels showing bending loss, large negative values denote large losses. Horizontal and oblique waveguides are connected without any adjustment in **b**. One waveguide (horizontal) has an extension of 1.0*a* in **c**. Both waveguides have equal extensions of 0.5*a* in **d**. **e**,**f**, Schematic structures and bending losses of the connecting parts of oblique waveguides and horizontal waveguides, respectively.

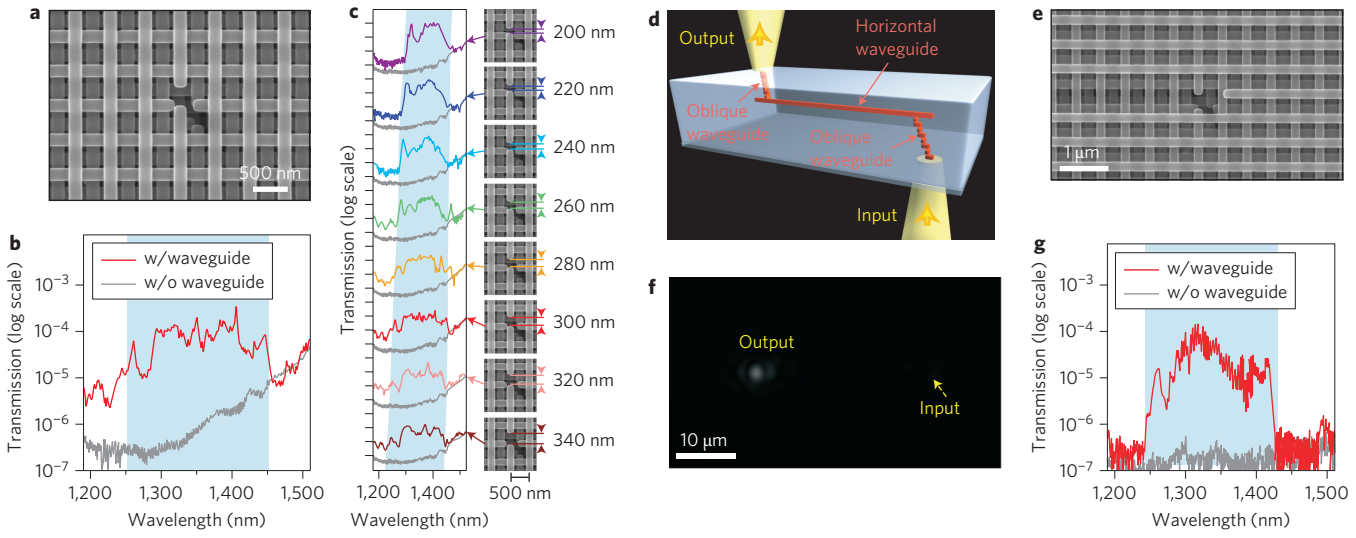

Figure 3 | Demonstration of light guiding in an oblique waveguide and connected oblique–horizontal–oblique waveguides. a,**b**, SEM image of the fabricated oblique waveguide and the measured transmission spectra. **c**, Dependence of guiding-band range on the constituent point-defect size of the oblique waveguide. Insets to **c**: SEM images of each waveguide. **d**, Schematic image of the connected oblique, horizontal and oblique waveguides. **e**, SEM image of the connecting point of the oblique and horizontal waveguides. **f**, Top-view optical microscope image of light guiding through the connected waveguides shown in **d**, where the incident wavelength is 1,337 nm. **g**, Measured transmission spectra of the connected waveguides.

of $a = 500$ nm to realize efficient bending, as shown in Fig. 2c.) The light transmission measurement was performed using a near-infrared camera, and the result is shown in Fig. 3f, with the length of the horizontal waveguide set at ~30 μm. The incident light was successfully transmitted through the oblique–horizontal–oblique waveguides. Figure 3g shows the measured transmission spectrum; the bandwidth and intensity are similar to those for the oblique waveguide alone, indicating that wideband connections have been realized between the waveguides.

We then constructed more sophisticated structures (Fig. 4a,d,g). In Fig. 4a, light is initially coupled into an oblique waveguide from the bottom side of the crystal, which is then connected to a horizontal waveguide. The light turns into a right-angled horizontal waveguide, is connected to another oblique waveguide, and is emitted

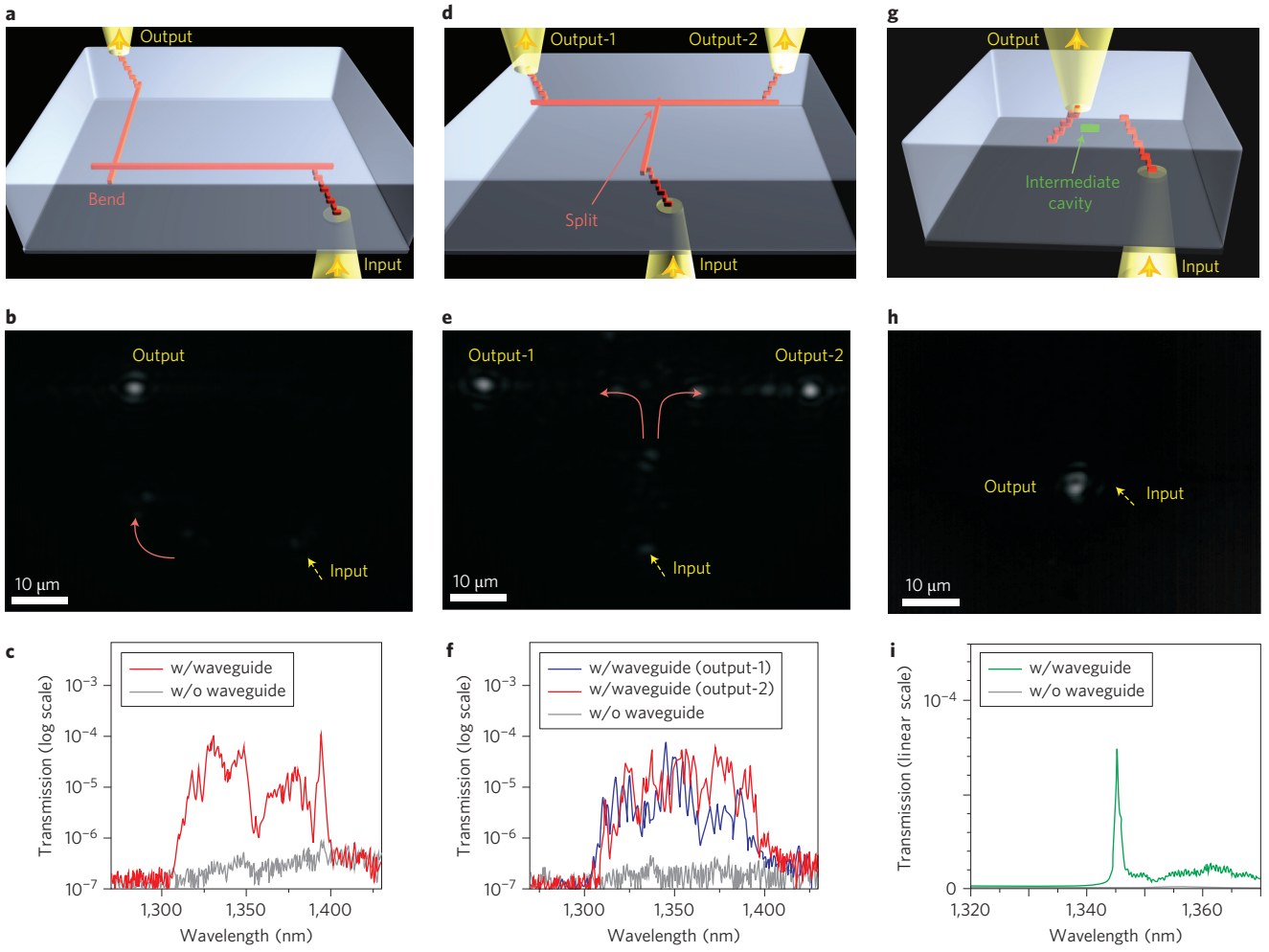

Figure 4 | Light guiding in sophisticated 3D guiding structures. a, Schematic of the structure including a right-angled connection of horizontal waveguides. **b**,**c**, Top-view optical microscope image (**b**) with incident wavelength of 1,349 nm, and transmission spectrum (**c**) of light propagation through a right-angled bend. **d**, Schematic of the structure with a light-splitting component. **e**,**f**, Optical microscope image (**e**) with incident wavelength of 1,354 nm, and transmission spectra (**f**) of propagation through the light-splitting part. **g**, Schematic of light guiding through an intermediate point-defect cavity. **h**,**i**, Optical microscope image (**h**) with incident wavelength of 1,345 nm, and transmission spectrum (**i**) of light propagation mediated by a cavity, respectively.

out of the crystal. For the connecting structures of the horizontal waveguides, extensions of 175 nm (= 0.35*a*) were introduced into both (Fig. 2f). The optical microscope image and the spectrum of the optical transmission through the structure are shown in Fig. 4b,c. For the case shown in Fig. 4d, light is further split into two, before being emitted out of the crystal. The split structure was constructed by extending one horizontal waveguide in the right-angled bending structure shown in Fig. 4a. The transmission optical microscope image and spectra from the two output ports of this arrangement are shown in Fig. 4e,f, which shows that the splitting of the light has been successfully realized. In Fig. 4g, two oblique waveguides are connected through an intermediate nanocavity (with a maximum quality factor of ~1,650 determined by 16 stacked-stripe layers), which was formed by introducing a point defect composed of a partially missing stripe, the width of which was designed to be 600 nm (= 1.2*a*). The optical transmission image and spectrum for this are shown in Fig. 4h,i. Thus, various demonstrations of the sophisticated 3D manipulation of photons have been successfully provided using the combination of our design strategy and fabrication technology.

In summary, we have demonstrated 3D optical-guiding phenomena in 3D photonic crystals by establishing systematic design principles for 3D waveguides and bends, in combination with the development of large-area silicon 3D photonic crystals based on an automatic alignment and stacking method. This achievement in the arbitrary 3D manipulation of photons will open the door to enhanced functionality, including sophisticated 3D photonic nanodevices/systems combined with nonlinearity, biophotonics, optomechanics and quantum-information processing. The goal of realizing ultimate photon control is now approaching.

Received 12 September 2012; accepted 4 December 2012; published online 20 January 2013

References

1. Noda, S., Tomoda, K., Yamamoto, N. & Chutinan, A. Full three-dimensional photonic bandgap crystals at near-infrared wavelengths. *Science* **289,** 604–606 (2000).
2. Ogawa, S., Imada, M., Yoshimoto, S., Okano, M. & Noda, S. Control of light emission by 3D photonic crystals. *Science* **305,** 227–229 (2004).
3. Qi, M. *et al.* A three-dimensional optical photonic crystal with designed point defects. *Nature* **429,** 538–542 (2004).
4. Imada, M., Lee, L-H., Okano, M., Kawashima, S. & Noda, S. Development of three-dimensional photonic-crystal waveguides at optical-communication wavelengths. *Appl. Phys. Lett.* **88,** 171107 (2006).
5. Rinne, S. A., García-Santamaría, F. & Braun, P. V. Embedded cavities and waveguides in three-dimensional silicon photonic crystals. *Nature Photon.* **2,** 52–56 (2008).
6. Aoki, K. *et al.* Coupling of quantum-dot light emission with a three-dimensional photonic-crystal nanocavity. *Nature Photon.* **2,** 688–692 (2008).
7. Ishizaki, K. & Noda, S. Manipulation of photons at the surface of three-dimensional photonic crystals. *Nature* **460,** 367–370 (2009).

8. Takahashi, S. *et al.* Direct creation of three-dimensional photonic crystals by a top-down approach. *Nature Mater.* **8,** 721–725 (2009).
9. Kawashima, S., Ishizaki, K. & Noda, S. Light propagation in three-dimensional photonic crystals. *Opt. Express* **18,** 386–392 (2010).
10. Staude, I., von Freymann, G., Essig, S., Busch, K. & Wegener, M. Waveguides in three-dimensional photonic-bandgap materials by direct laser writing and silicon double inversion. *Opt. Lett.* **36,** 67–69 (2011).
11. Chutinan, A. & John, S. Light localization for broadband integrated optics in three dimensions. *Phys. Rev. B* **72,** 161316(R) (2005).
12. Chutinan, A. & John, S. 3+1 dimensional integrated optics with localized light in a photonic band gap. *Opt. Express* **14,** 1266–1279 (2006).
13. Chutinan, A. & Noda, S. Highly confined waveguides and waveguide bends in three-dimensional photonic crystal. *Appl. Phys. Lett.* **75,** 3739–3741 (1999).
14. Li, Z-Y. & Ho, K-M. Waveguides in three-dimensional layer-by-layer photonic crystals. *J. Opt. Soc. Am. B* **20,** 801–809 (2003).
15. Kawashima, S., Lee, L-H., Okano, M., Imada, M. & Noda, S. Design of donor-type line-defect waveguides in three-dimensional photonic crystals. *Opt. Express* **13,** 9774–9781 (2005).
16. Mekis, A. *et al.* High transmission through sharp bends in photonic crystal waveguides. *Phys. Rev. Lett.* **77,** 3787–3790 (1996).
17. Chutinan, A., Okano, M. & Noda, S. Wider bandwidth with high transmission through waveguide bends in two-dimensional photonic crystal slabs. *Appl. Phys. Lett.* **80,** 1698–1700 (2002).
18. Pile, D. F. P. & Gramotnev, D. K. Plasmonic subwavelength waveguides: next to zero losses at sharp bends. *Opt. Lett.* **30,** 1186–1188 (2005).
19. Yamamoto, N., Noda, S. & Chutinan, A. Development of one period of a three-dimensional photonic crystal in the 5–10 μm wavelength region by wafer fusion and laser beam diffraction pattern observation techniques. *Jpn J. Appl. Phys.* **37,** L1052–L1054 (1998).
20. Kawashima, S., Imada, M., Ishizaki, K. & Noda, S. High-precision alignment and bonding system for the fabrication of 3-D nanostructures. *J. Microelectromech. Syst.* **16,** 1140–1144 (2007).

Acknowledgements

The authors thank Y. Tanaka and T. Asano for fruitful discussions and helpful advice. This work was partly supported by JST, CREST, by Kyoto University G-COE, by a Grant-in-Aid for Scientific Research from JSPS, and by METI.

Author contributions

S.N. supervised the entire project. K.I. and M.K. analysed 3D guiding structures. K.I., together with K.S. and K.G., fabricated the samples. K.I., M.K. and K.G. measured the 3D optical guiding phenomena. S.N., K.I. and M.K. discussed the results. S.N and K.I. wrote the manuscript.

Additional information

Supplementary information is available in the online version of the paper. Reprints and permission information is available online at http://www.nature.com/reprints. Correspondence and requests for materials should be addressed to S.N.

Competing financial interests

The authors declare no competing financial interests.